Innate Tissue Fluorescence of the Oral Mucosa of Controls and Head and Neck Cancer Patients

Howard E. Savage
Venkateswara Kolli
John Ansley
Rajiv Y. Chandawarkar
Robert R. Alfano
Stimson P. Schantz

Memorial Sloan-Kettering Cancer Center
Department of Surgery, Head and Neck
Service, New York, NY, 10021
(H.E.S, V.K., J.A., R.Y.C., S.P.S.)

City College of the City University of New York
Mediphotonic Laboratory, Institute for Ultrafast Lasers
New York, NY 10031
(R.R.A.)

ABSTRACT

Base line spectral excitation and emission scans were defined for the oral mucosa in a population of 61 controls, 16 oral tongue cancer patients and 2 patients with tongue leukoplakia. A xenon-based fluorescence spectrophotometer (Mediscience Corp.) with a fiberoptic probe (Mediscience Corp.) was used to collect excitation and emission spectra. Two excitation scans (λEx 200-360nm, λEm 380nm; λEx 240-430nm, λEm 450nm) and two emission scans (λEx 300nm, λEm 320-580nm; λEx 340nm, λEm 360-660nm) were used to analyze the buccal mucosa (BM), hard palate (HP), floor of mouth (FOM) and dorsal tongue (DT) of 61 control individuals. In 41 controls the lateral tongue site (LT) was added. The same set of scans was performed on tumor lesions and contralateral normal tissues of 16 patients with lateral tongue tumors and on two individuals with leukoplakia of the tongue. Ratios of points on the individual scans were used to quantitate data. The excitation scan (λEx 200-360nm, λEm 380nm) and the emission scan (λEx 300nm, λEm 320-580nm) were able to statistically discriminate the HP and DT from the BM and FOM. The ratios of intensities of neoplastic mucosa and contralateral sites were significantly different with the excitation scans (λEx 200-360nm, λEm 380nm, $p < 0.001$) and (λEx 240-430nm, λEm 450nm, $p < 0.01$) and with the emission scan (λEx 300nm, λEm 320-580nm, $p< 0.001$). Discrimination was significant with the emission scan (λEx 340nm, λEm 360-660nm, $p < 0.07$). Innate tissue fluorescence has potential as a monitor of cancer patients and populations at risk for head and neck cancer.

0-8194-1734-3/95/$6.00

KEYWORDS: tissue fluorescence, oral mucosa, head and neck cancer, diagnostics, optical biopsy

2. INTRODUCTION

Innate cellular and tissue fluorescence, has been investigated as a novel diagnostic tool for the identification of preneoplastic and neoplastic tissue. Its relevance to clinical oncology include use as an intermediate endpoint biomarker in cancer chemoprevention trials[1]. Different organ systems have been investigated both *in vivo* and *in vitro* using this technology and include the lung[2,3], colon[4-7], skin[8], heart[9], breast[10], ovary[11] and cervix[12]. The fluorescence patterns of single cells have also been studied[13]. The underlying basis for such investigations is that fluorescence is strongly influenced by intra and extra cellular molecules found in cells and tissues. These include flavins, aromatic amino acids, nicotinamide adenine dinucleotide (NADH), and collagen, all of which fluoresce in the ultraviolet and visible regions of the light spectrum[14,15]. Tissues in varying stages of progression towards malignancy should differ from normal tissues in both the qualitative and quantitative nature of these intrinsic cellular fluorophores. The examination the fluorescent characteristics of such intrinsic cellular and tissue fluorophores has provided information about tissue microstructure and the changes therein without interfering with the native cellular environment[5,6,16].

Multiple excitation sources have been utilized in the detection of native cellular fluorescence, including argon[2,10], krypton[2], helium-cadmium[2,3,7,8], and pulsed-nitrogen lasers[4-6,12]. The instrumentation used in this study is a xenon lamp based fluorescence spectrometer, CD-scan (Mediscience Technology, Cherry Hill, NJ). Using this instrument, both excitation and emission spectra can be obtained from cells and tissue samples. The applicability of tissue autofluorescence analysis was tested on control and head and neck patient populations using this fluorescence spectrometer design and current bioptical technology.

3. METHODS

3.1 Control and patient population

The control population included 61 individuals. Fifty-three were healthy hospital volunteers and 8 were cancer patients with cancer at a site other than the oral cavity. There were 27 males and 34 females. Their ages ranged from 24-74 years. They were further divided into three groups depending on their smoking status: current smokers (n = 15), non-smokers (n = 36) and past smokers (n = 10).

The oral tongue patients numbered 18 total. Sixteen were patients with squamous cell carcinoma of the lateral tongue and 2 had leukoplakia of the tongue. There were 13 males and 5 females.

Their ages ranged from 33-86 years. Significantly, 16 of these individuals were still smokers and 2 were non-smokers. There were no past smokers in this group.

3.2 Autofluorescence analysis

3.21 Instrumentation

The control and patient population were scanned using a hand held, quartz fiber optic probe attached to a fluorescence spectrophotometer (Mediscience Technology Corporation CD Scanner). The probe is six feet long with an inner diameter of three mm. The fibers in the probe are randomly bifurcated with half going to the excitation and half to the emission side of the the spectrophotometer. The the optical fibers are recessed 3 mm in a stainless steel sleeve at the tip of the probe to prevent contract with the mucosal surface and to prevent extrinsic white light from interfering with the fluorescence. The probe is disinfected for thirty minutes before each use with a Cidex solution (Johnson and Johnson, Medical Inc. Arlington, TX) and then washed extensively to remove any contaminating Cidex. A rhodamine correction curve is stored within the instrument to correct for the response of the reference photomultiplier. Instrument calibration is also checked on a monthly basis using an ovalene standard (Starna Cells, Inc. Atascadero, CA).

3.22 Data analysis

All the scans will be identified first by their excitation wavelength, followed by the specific emission wavelength. Emission scans were performed by exciting the tissues at one particular wavelength while the emission was measured over a variable wavelength. Conversely, the excitation scans were performed by exciting the tissues with a variable wavelength while the emission was measured at a fixed wavelength. Two emission scans (λEx 300nm, λEm 320-580nm; λEx 340nm, λEm 360-660nm) and two excitation scans (λEx 200-360nm, λEm 380nm; λEx 240-430nm, λEm 450nm) were used in this study. These scans were chosen because they had shown consistent differences in our previous studies using an n-nitroso-methylbenzylamine (NMBA) rat esophageal tumor model and a retinoic acid treated multicellular tumor spheroid model[16,17]. These scans also bracket the emission and excitation maxima of the major intra and extra cellular fluorophores.

In the control population, the four different fluorescence analyses, two emission scans, λEx 300nm, λEm 320-580nm; λEx 340nm, λEm 360-660nm) and two excitation scans (λEx 200-360nm, λEm 380nm; λEx 240-430nm, λEm 450nm, were performed at each of four sites (HP = hard pallate, DT = dorsal tongue, BM = buccal mucosa and FOM = floor of mouth) within the oral cavity for all of the 61 controls. Later, a fifth site, the lateral tongue, (LT) was added so that 41 of the 61 controls also had this site

scanned. The scans were analyzed using the ratio method as described by Profio *et al* and used by Hung *et al*[18,19]. The following ratios were used for the individual scans: 340nm/440nm for the emission scan, λEx 300nm, λEm 320-580nm; 450nm/585nm for the emission scan,λEx 340nm, λEm 360-660nm; 300nm/325nm for the excitation scan, λEx 200-360nm, λEm 380nm; and 335nm/375nm for the excitation scan, λEx 240-430nm, λEm 450nm. Area under the curve between the wavelengths 300-400nm was also used to quantitate the excitation scan, λEx 240-430nm, λEm 450nm.

In the tongue patient group, the four scan analyses were done on the patients' lesion and then on the contralateral normal site for a paired comparison. The scans analyzed as described above. This data was then analyzed using the paired t-test. Statistical analysis of control and patient data was done using Minitab statistical software package (Minitab, Inc., State College, PA).

4. RESULTS

4.1 Controls

Figure 1A-1D shows representative emission scans (λEx 300nm, λEm 320-580nm; λEx 340nm, λEm 360-660nm) and excitation scans (λEx 200-360nm, λEm 380nm; λEx 240-430nm, λEm 450nm) comparing the buccal mucosa and the dorsal tongue of one healthy normal control. Group data is shown in Tables I and II. Table I illustrates the analysis of variance of the two emission scans for the 61 control individuals at the five sites analyzed. Note that only 41 individuals were analyzed at the LT site. The 95% confidence intervals for the different group sites is represented by the mean ratio value $\pm$ two standard errors of the mean of the ratios. In the emission scan λEx 300nm, λEm 320-580nm, the BM and FOM had similar mean ratio values while the HP, DT and LT grouped together with overlaping 95% confidence interals. Of all of the scans analyzed the emission scan, λEx 340nm, λEm 360-660nm, demonstrates the greatest overlap of the 95% confidence interval for the mean ratios with the DT, BM and FOM grouping together and the HP and LT grouping together. Table II depicts the analysis of variance for the two excitation scans for the 61 controls at the five sites analyzed. In the analysis of variance of the excitation scan, λEx 200-360nm, λEm 380nm, the the HP and DT grouped together and the BM and FOM grouped together with the LT having a 95% confidence that falls in between the two groups. In the excitation scan, λEx 240-430nm, λEm 450nm, the 95% confidence interval of the 335/375 nm ratio are similar for the BM and FOM with the HP now falling in this grouping while the DT and LT now fall into a similar grouping. Clearly, the sites have differences in the means of their ratios of intensities in the four scans. This result was not surprising since these sites within the oral cavity differ in their histology, states of differeniation, metabolism and proliferation rates. Figure 2, is a histogram of the actual individual data points for the

excitation scan, λEx 200-360nm, λEm 380nm. The DT, BM and FOM have normal distributions, however, with the available data, it is not clear if the HP and LT will have a normal or biphasic distribution of data points.

4.2 Lateral tongue tumor verses contralateral normal

Figures 3A-3D, represent the tumor verses contralateral normal comparison of one lateral tongue tumor patient. The group paired data comparisons are shown in Table III. Using ratio of intensities as the measurement, the lateral tongue tumors are seen to be significantly different from the contralateral normal tissue in three of the four scans while the emission scan, λEx 340nm, λEm 360-660nm, only approaches significance ($p = 0.07$).

5. DISCUSSION

Several emission and excitation spectra have been used to differentiate normal from preneoplastic and malignant tissues. Using *in vitro* tissues, Alfano *et al* used the ratio of intensities of 340 to 440nm wavelengths in the emission spectra (λex 300nm, λem 320-580nm) to discriminate malignant tumor, benign tissue, and normal tissue of the breast, cervix and ovary. They found that malignant tumor had the highest ratio and normal tissue had the lowest ratio[10,11,20,21]. One scan that currently differentiates tumor, preneoplastic and tumor tissues is the emission scan that runs from 300 nm to 700-800nm, with excitation wavelengths generated from a pulsed nitrogen laser (λex 337nm)[4-6,12] or a helium-cadmium laser (λex 325nm)[2,3,7,8]. The biological nature for the differences seen in this particular scan for tumor and normal tissue is thought due to the loss of the spectral signal from collagen[5,16]. Lam *et al* use a krypton ion (λex 405nm), helium-cadmium (λex 442nm), and argon laser (λex 488nm) to investigate the *in vivo* emission of lung tissues in the range of 480 to 700nm. With these laser excitation wavelengths, emission light is lost over the entire emission range when comparing normal lung tissue to carcinoma *in situ*. The loss of green fluorescence in the tumor is thought to be the result of the differences in the amounts of oxidized and reduced flavins in the tumor tissue[3]. The fluorescent patterns observed in the multiple scans performed in this study represent the summation of the fluorescence intensities of many intrinsic cellular fluorophores[14,15]. The fluorescence patterns will be dominated by those biomolecules which absorb and emit at the wavelengths covered by the emission and excitation scans used. Based on fluorescent patterns of known biomolecules, the excitation scan, λEx 300nm, λEm 320-580nm is dominated by emission from the aromatic amino acids tyrosine, tryptophan and phenylalanine, collagen, elastin, NADH and FAD. The emission scan, λEx 340nm, λEm 360-660nm covers the emission range of collagen, elastin, NADH and FAD. The excitation scan, λEx 200-360nm, λEm 380nm would include the excitation maxima for the aromatic amino acids,

nucleic acids and collagen and the excitation scan, λEx 240-430nm, λEm 450nm would cover mainly NADH, collagen and elastin. Both NADH and FAD fluorescent levels within cells are dependent on the presence of oxygen. Chance *et al* have shown that changes in the relative amounts of oxygen in cell systems will be reflected in altered levels of NADH and FAD fluorescence, within two to three minutes[22,23]. Chance *et al* have shown that within tumor tissue slices there are different levels of NADH fluorescence at different locations either near or distant to blood vessels. This was thought to be reflective of the oxygenation of the tissue NADH at the location scanned[24].

The scans with the most discriminatory capacity in this study were the excitation scans, λex 200-360nm, λem 380nm and λEx 240-430nm, λEm 450nm and the emission scan, λEx 240-430nm, λEm 450nm. The emission scan, λEx 340nm, λEm 360-660nm, while approaching significance in differentiating tongue lesions from contralateral normal tissue, was the least discriminatory. This is of note as previous researchers have shown this to be a very effective scan[2-8,12].

While lasers can generate more light energy, they are restricted to a single excitation wavelength. For identification of those molecules responsible for the differences seen between normal, preneoplastic and tumor cells, an instrument that can identify both emission and excitation maxima is advantageous. Clearly, an excitation scan that identifies a molecule whose fluorescence is lost or gained should have a confirmatory emission scan the shows a similar change. In fact, this was the case in our NMBA animal model where the loss of collagen signal was verified by the loss of signal at 390 nm in the emission scan, λex 340nm, λem 360-660nm and a concomitant loss of signal at 330nm in the excitation scan, λex 200-360nm, λem 380nm[16]. Both the emission maxima and excitation maxima matched those of collagen. The discriminatory excitation scans used in this study may represent another set of scans that can be added to the list of those used in the development of optical imaging of tumors. The best imaging systems may have to rely on both multiple emission and excitation scans for optimal resolution of tumor.

Native tissue fluorescence is being investigated as a potential intermediate endpoint biomarker. In the present study, correlations between tissue autofluorescence and cellular proliferation have been identified. The establishment of non-invasive methods which reflect altered proliferation, differentiation and histoarchitecture major components of dysplasia and premalignancy support our aim in developing this technology.

6. REFERENCES

1. S. P. Schantz and R. R. Alfano, Tissue autofluorescence as an intermediate endpoint in cancer chemoprevention trials. J. of Cell. Biochem., 17F:199-204, 1993.
2. J. Hung, S. Lam, J. C. LeRichie and B. Palcic, Autofluorescence of normal and malignant bronchial tissue. Lasers in Surg. Med. 11:99-105, 1991.
3. S. Lam, C. MacAulay, J. Hung, J. LeRichie, A. E. Profio, and B. Palcic, Detection of dysplasia and carcinoma in situ with a lung imaging fluorescence endoscope device. J. Thoracic Cardiovascular Surg. 105:1035-1040, 1993.
4. R. M. Cothren, R. Richards-Kortum, M. Sivak, M. Fitzmaurice, R. P. Rava, G. A. Boyce, M. Doxtader, R. Blackman, T. B. Ivanc, G. B. Hayes, M. S. Feld and R. E. Petras, Gastrointestinal tissue diagnosis by laser-induced fluorescence spectroscopy at endoscopy. Gastrointest. Endosco. 36:105-111, 1990.
5. K. T. Schomacker, J. K. Frisoli, C. C. Compton, T. J. Flotte, J. M. Richter, N. S. Nishioka and T. F. Deutsch, Ultraviolet laser-induced fluorescence of colon tissue: basic biology and diagnostic potential. Laser Surg. Med. 12:63-78, 1992.
6. K. T. Schomacker, J. K. Frisoli, C. C. Compton, T. J. Flotte, J. M. Richter, T. F. Deutsch and N. S. Nishioka, Ultraviolet laser-induced fluorescence of colonic polyps. Gastroenterol. 102:1155-1160, 1992.
7. C. R. Kapadia, F. W. Cutruzzola, K. M. Obrien, M. L. Stetz, R. Enriquez and L. I. Deckelbaum, Laser induced fluorescence spectroscopy on human colonic mucosa. Gastroenterol. 99:150-157, 1990.
8. D. J. Leffell, M. L. Stetz, L. M. Milstone and L. I. Deckelbaum, In vivo fluorescence of human skin. Arch. Derm. 124:1514-1518, 1988.
9. C. Ince, J. F. Ashruf, E. A. Sanderse, E. G. J. M. Pierik, J. M. C. C. Coremans and H. A. Bruining, In vivo NADH and Pd-porphyrin video fluori-/phosphorimetry. *In*: W. Erdman and D. F. Bruley (eds.), Advances in Experimental Medicine and Biology, Vol XIV, pp. 267-275. New York: Plenum Press, 1992.
10. R. R.Alfano, A. Pradhan and G. C. Tang, Optical spectroscopic diagnosis of cancer and normal breast tissues. J. Opt. Soc. Am. B, 6:1015-1023, 1989.
11. B. B. Das, W. S. Glassman, R. R. Alfano, J. Cleary, R. Prudente, E. Celmer and S. Lubicz, UV fluorescence spectroscopic technique in the diagnosis of breast, ovarian, uterus and cevix cancer. SPIE 1427:368-373, 1991.
12. N. Ramanujam, M. F. Mitchell, A. Mahadevan, S. Thomsen, E. Silva and R. Richards-Kortum, Fluorescence spectroscopy: A diagnostic tool for cervical intraepithelial neoplasia (CIN). Gyn. Oncol. 52:31-38, 1994.

13. J. Eng, R. M. Lynch, and R. S. Balaban, Nicotinamide adenine dinucleotide fluorescence spectroscopy and imaging of isolated cardiac myocytes. Biophys. J. 55:621-630, 1989.
14. S. Undenfriend, Fluorescence assays in biology and medicine. Vol. 1, New York, Academic Press, 1962.
15. S. Undenfriend, Fluorescence assays in biology and medicine. Vol. 2, New York, Academic Press, 1969.
16. R. Glasgold, M. Glasgold, H. E. Savage, J. Pinto, R. R. Alfano, S. P. Schantz, Tissue autofluorescence as an intermediate endpoint in NMBA-induced esophageal carcinogenesis. Cancer Lett. 85:223-232, 1994.
17. M. B. Silberberg, H. E. Savage, G. C. Tang GC, P. G. Sacks, R. R. Alfano and S. P. Schantz, Detecting retinoic acid induced biochemical alterations in squamous cell carcinoma using intrinsic fluorescence spectroscopy. Laryngoscope 104:278-283, 1994.
18. A. E. Profio and O. J. Balchum, Fluorescence diagnosis of Cancer. In: D. Kessel, Ed. Proceedings of the Pophyrin Photosensitization Workshop, July 6-7, 1984. New York: Plenum Press, 1985;43-50.
19. J. Hung, S. Lam, J. C. LeRichie, and B. Palcic, Autofluorescence of normal and malignant bronchial tissue. Laser Surg Med.11:99-105, 1991.
20. W. S. Glassman, C. H. Lui, G. C. Tang, S. Lubicz, R. R. Alfano, Ultraviolet excited fluorescence spectra from non-malignant and malignant tissue of the gynecological tract. Laser Life Sci. 1:1-9, 1991.
21. D. B. Tata, M. Foresti, J. Cordero, P. Tomashefsky, M. A. Alfano and R. R. Alfano, Fluorescence polarization spectroscopy and time-resolved fluorescence kinetics of native cancerous and normal rat kidney tissues. Biophysio. J. 50:463-469, 1986.
22. B. Chance, B. Schoener, R. Oshino, F. Itshak and Y. Nakase, Oxidation-reduction ratio studies of mitochondria in freeze-trapped samples. NADH flavoprotein fluorescent signals. J. Biol. Chem. 254:4764-4771, 1979.
23. B. Chance, P. Cohen, F. Jobis and B. Schoener, Intracellular oxidation-reduction rates *in vivo*. The microfluorometry of pyridine nucleotide gives a continuous measure of the oxidation state. Science 137:499-508, 1962.
24. M. Gosalvez, R. G. Thurman, B. Chance and H. S. Reinhold, Indication of hypoxic areas in tumors from in vivo NADH fluorescence. Europ. J. Cancer 8:267-269, 1972.

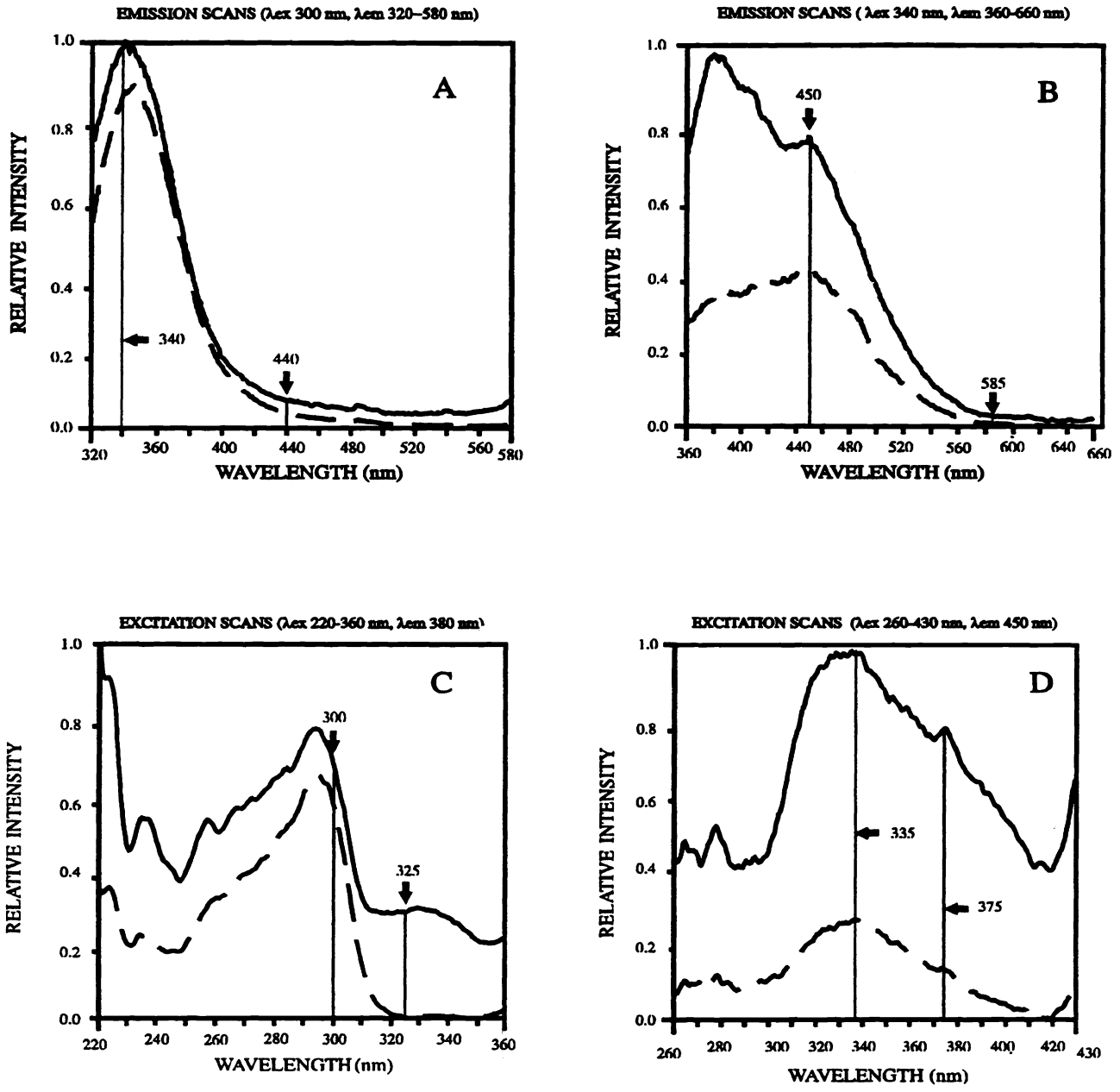

Figure 1. Excitation and emission scans of one representative control individual. Emission scans, λex 300 nm, λem 320-580 nm (A) and λex 340 nm, λem 360-660 nm (B). Excitation scans λex 220-360, λem 380 nm (C) and λex 260-660 nm, λem 450 nm (D). Solid line is the scans of the buccal mucosa and dotted line is the scans of the dorsal tongue.

Table I

EMISSON SCANS ANALYSIS OF VARIANCE

λex 300nm, λem320-580nm; ratio 340/440nm

LEVEL	N	MEAN	STDEV
HP300	61	20.645	4.767
DT300	61	18.246	4.997
BM300	61	13.651	3.368
FOM300	61	13.409	5.508
LT300	41	19.221	5.013
POOLED STDEV =		4.769	

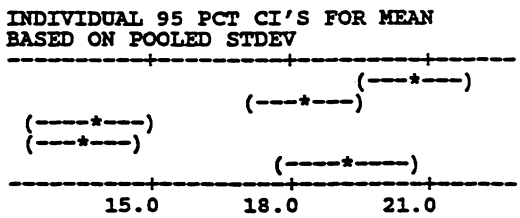

λex 340nm, λem 360-660nm; ratio 450/585nm

LEVEL	N	MEAN	STDEV
HP340	61	21.420	5.371
DT340	61	19.071	4.312
BM340	61	18.354	3.988
FOM340	61	18.692	4.581
LT340	41	21.492	5.704
POOLED STDEV =		4.766	

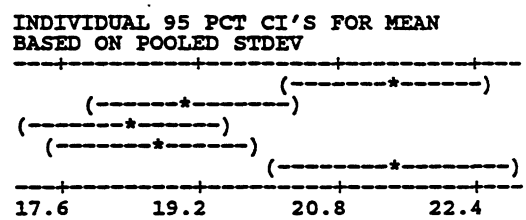

Table II

EXCITATION SCANS ANALYSIS OF VARIANCE

λex 260-360nm, λem 380nm; ratio 300/325nm

LEVEL	N	MEAN	STDEV
HP380	61	6.483	3.158
DT380	61	5.833	1.536
BM380	61	3.320	0.840
FOM380	61	2.821	1.050
LT380	41	4.708	1.464
POOLED STDEV =		1.826	

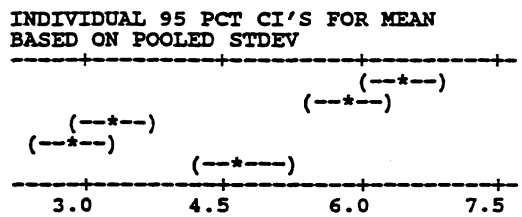

λex 260-430nm, λem 450nm; ratio 335/375nm

LEVEL	N	MEAN	STDEV
HP450	61	1.2603	0.1218
DT450	61	1.4220	0.1045
BM450	61	1.2195	0.1302
FOM450	61	1.2705	0.2229
LT450	41	1.4676	0.1739
POOLED STDEV =		0.1553	

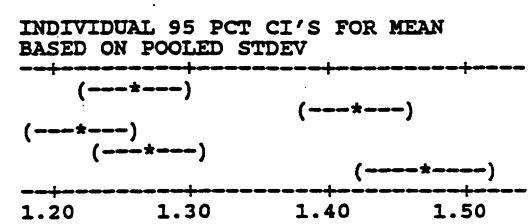

HP = hard pallate, DT = dorsal tongue, BM = buccal mucosa, FOM =floor of mouth, LT = lateral tongue

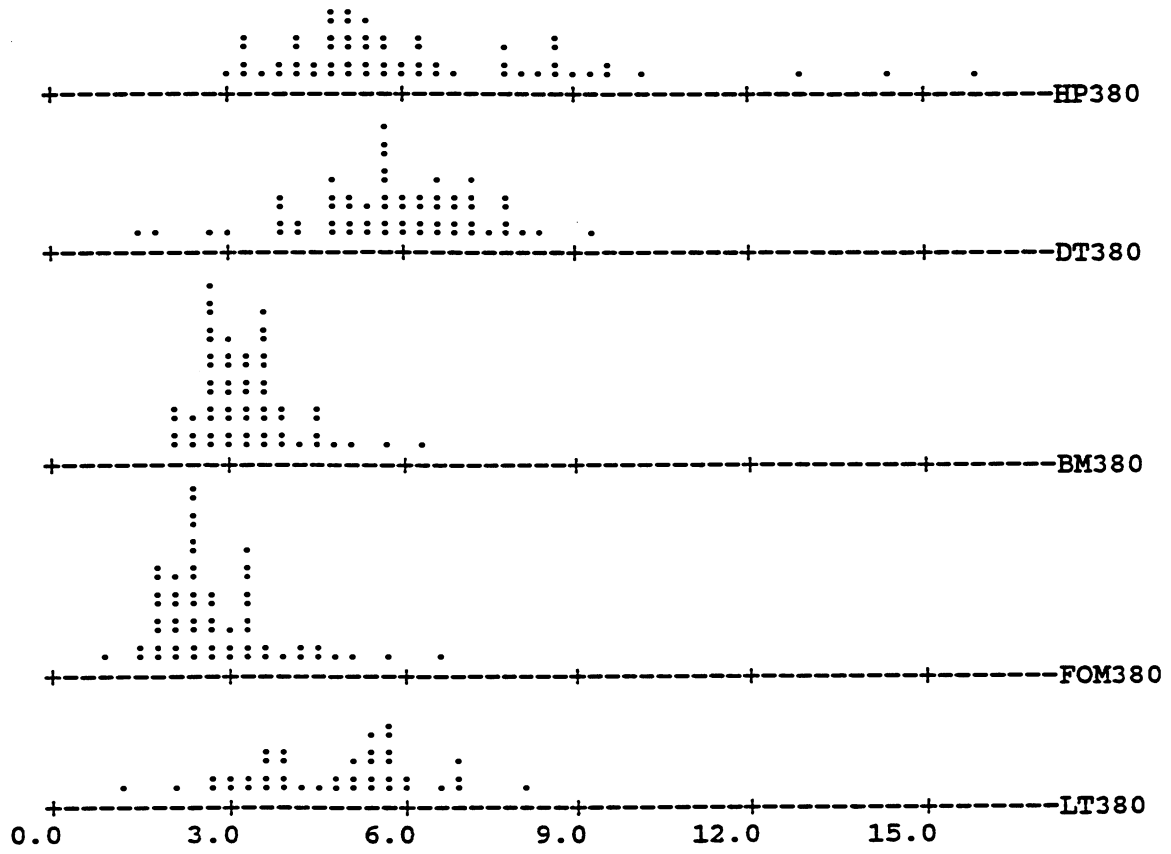

Figure 2. Histogram of each ratio data point of for the excitation scan λex 220-360 nm, λem 380nm for the hard pallate (HP), dorsal tongue (DT), buccal mucosa (BM), floor of mouth (FOM) and lateral tongue (LT).

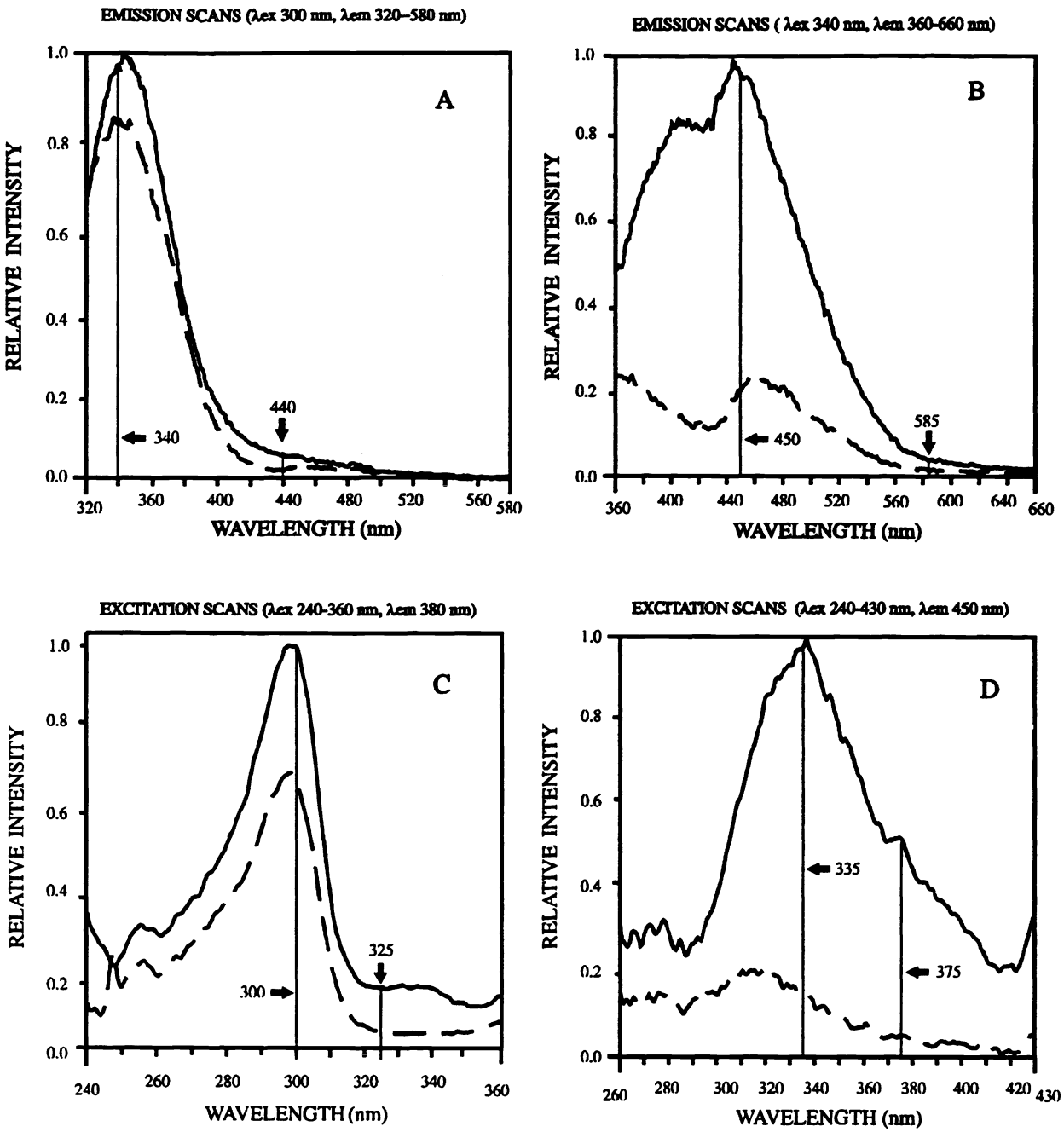

Figure 3. Excitation and emission scans of one lateral tongue tumor patient. Emission scans λex 300 nm, λem 320-580 nm (A) and λex 340 nm, λem 360-660 nm (B). Excitation scans λex 220-360 nm, λem 380 nm (C) and λex 260-430 nm, λem 450 nm (D). The tumor scans have dotted lines and the contralateral normal tissue have solid lines.

TABLE III

SCANS	RATIOS OF INTENSITIES	NORMAL	TUMOR
λEx 300nm, λEm 320-580nm	340/440	15.66 ± 1.30	23.84 ± 1.30[1]
λEx 340nm, λEm 360-660nm	450/585	22.71 ± 3.95	15.29 ± 1.34[2]
λEx 200-360nm, λEm 380nm	300/325	3.57 ± 0.36	5.46 ± 0.34[3]
λEx 240-430nm, λEm 450nm	335/375	1.36 ± 0.06	1.48 ± 0.07[4]
	Area	4816 ± 805	2919 ± 552[5]

p values of tumor verses normal ratio: [1]< 0.001, [2]< 0.07, [3]< 0.001, [4]< 0.01 and [5]< 0.001.

Number of individuals out of the total number who demonstrated the same trend from normal to tumor: [1]ratio increase 18/18, [2]ratio decrease 13/18, [3]ratio increase 15/18, [4] ratio increase 14/18 and [5]area under the curve decrease 17/18.

[5]Area under the curve between 300-400nm.